PRAMANA
— journal of
physics

Vol. 69, No. 3
September 2007
pp. 459–465

Energy resolution methods efficiency depending on beam source position of potassium clusters in time-of-flight mass spectrometer

Ş ŞENTÜRK[1], F DEMİRAY[1,2] and O ÖZSOY[3]
[1]Department of Physics, Dumlupınar University, Kütahya 43100, Turkey
[2]Department of Physics, Gebze Institute of Technology, Gebze, Kocaeli, 41400 Turkey
[3]Bozantı Cd. # 114/13 Kayseri, 38020 Turkey
E-mail: osozsoy@gmail.com

MS received 17 November 2006; revised 9 May 2007; accepted 8 June 2007

Abstract. Energy resolution of the time-of-flight mass spectrometer was considered. The estimations indicate that the time-lag energy focusing method provides better resolution for the parallel case while the turnaround time is more convenient for the perpendicular position. Hence the applicability of the methods used for the energy resolution depends on beam source arrangement.

Keywords. Energy resolution; time-lag energy focusing method; turnaround time method; time-of-flight mass spectrometer.

PACS Nos 82.80.Rt; 87.57.Ce

1. Introduction

Besides the spatial resolution, the initial velocity compensation called energy resolution is essential to obtain better resolution for the time-of-flight (ToF) mass spectrometer. Application-wise, the ToF mass spectrometer has the beam source in a perpendicular position to the spectrometer axis [1–3]. In this way, the velocity component effect is minimized and hence the initial velocity is not compensated. This operation mode in turn accesses the information on quantities such as velocity and fragmentation.

For the spectrometer with the beam source along the axis, the velocity component causes poor resolution [4]. From the experimental point of view, the poor resolution limits mass range. However, direct beam experiment method indicates that the arrangement can improve the signal-to-noise ratio [5]. This is significant for studies which encounter low signal level [3]. In this report, the energy resolution for the ToF mass spectrometer was studied taking into account the beam source positions, the aim of which is to clarify the efficiency of the methods applied for the energy

resolution. The Wiley–McLaren-type geometry is utilized in a similar manner as the spectrometer geometry. In the following section, the principle of the spectrometer is explained. In §3, the methods for the energy resolution are given together with the results and we conclude in §4.

2. Principle of the spectrometer

2.1 *Description of the spectrometer*

The spectrometer has a beam source, ionization–acceleration and free-flight zones shown in figure 1 where the beam source positions are presented, namely along the spectrometer axis and perpendicular to the axis. The ionization–acceleration zone consists of regions A and B. In region A, the particles are ionized and they are pushed through region B by the electric field $\bar{E}_1$. The electric field $\bar{E}_2$ accelerates the ionized particles further. The region L is the free-flight zone where the accelerated particles drift freely. In this region the accelerated particles experience no electric field and ion packets of different masses are separated. The mass-separated particles then come to the grounded microchannel plates (MCP) detector.

2.2 *Time-of-flight calculation*

The total flight time of a particle having a mass m and charge q, starting from the initial distance x of the first grid with an initial velocity v along the spectrometer axis, will be the sum of three partial flight times (these are flight times in each region). The total flight time using the reduced parameter approach is given below eq. (1), where the reduced parameter approach simplifies the calculations, as

$$T(x,v) = L\sqrt{m/2qV}\, f(X,S), \tag{1}$$

where $f(X,S)$ is a dimensionless function and is given by

$$\begin{aligned} f(X,S) = &\left[\frac{2(\sqrt{S^2+EX}-S)}{E}\right] \\ &+\left[2b\left(\sqrt{S^2+EX+1}-\sqrt{S^2+EX}\right)\right] \\ &+\left[\frac{1}{\sqrt{S^2+EX+1}}\right]. \end{aligned} \tag{2}$$

In this function, $X = x/L$ is the reduced initial position of the particle, $S = v(m/2qV)^{1/2}$ is the reduced initial velocity, $b = B/L$ is the reduced length of region B and $E = (V_a/V)(L/A)$ is the reduced value of the electric field in region A. The notation of the parameters used here follows the studies of de Heer *et al* and Chandezon *et al* [6,7]. The function $f(X,S)$ defines the flight time for the spectrometer arrangement and values of the parameters of this function determine the properties of the spectrometer.

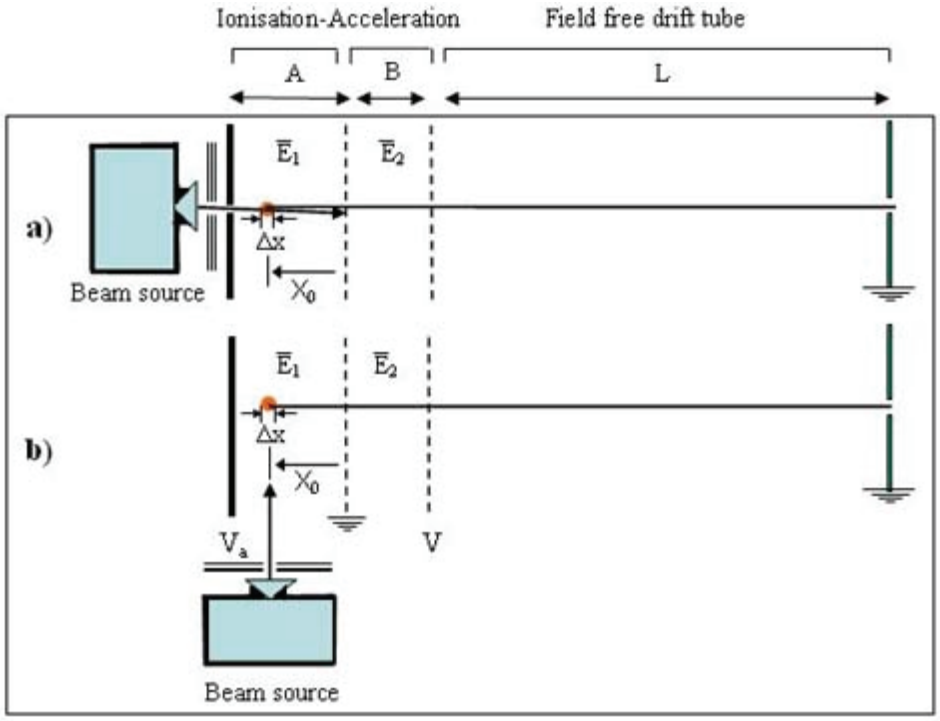

Figure 1. Block diagram of the ToF spectrometer. (**a**) Spectrometer with the cluster beam source along the axis. (**b**) Spectrometer with the cluster beam source perpendicular to the axis.

3. Energy resolution

Energy resolution is to compensate the initial velocity component effect of the mass resolution. The compensation is carried out via turnaround time and time-lag focusing methods [1], which were implemented for $f(X, S)$ and $f(X, S = 0)$. $f(X, S)$ defines the spectrometer with the beam source along the axis while $f(X, S = 0)$ is for the beam source perpendicular to the spectrometer axis.

3.1 *Turnaround time approach*

In the turnaround time method, two identical ions in the same position with the same initial kinetic energy, but with opposite velocities are considered [1]. The ion with opposite velocity needs a turnaround time to reach the detector compared to the ion with velocity along the detector direction. The expression for the turnaround time using eq. (1) is as follows:

$$\delta T_v = 2mv/qE_1, \tag{3}$$

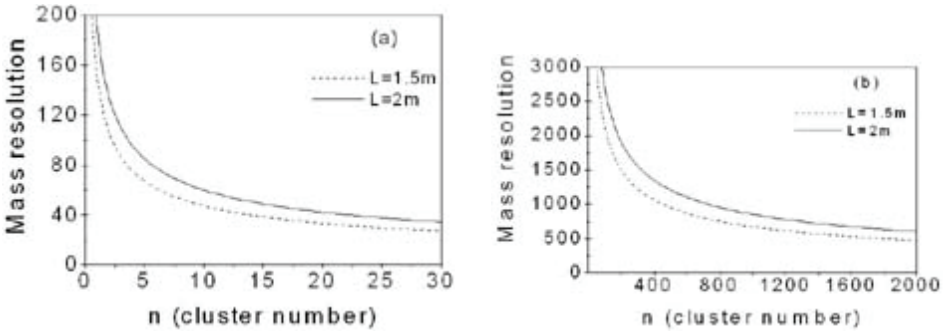

Figure 2. Mass resolution variation with the cluster size n. (**a**) Beam source parallel to the spectrometer axis and (**b**) beam source perpendicular to the axis.

where m, v and q are the mass, velocity and charge of the particle, respectively, and E_1 is the magnitude of the electric field in region A. The mass resolution with eqs (1) and (3) is

$$\left(\frac{m}{\delta m}\right)_v = \frac{1}{2}\frac{T}{\delta T_v} = \frac{LV_a\sqrt{q}f(X,S)}{vA\sqrt{32mV}}, \tag{4}$$

where V_a and V are the voltages for the acceleration plates, L and A are the lengths for the free flight region and ionization region, mass m and charge q belong to the particle and $f(X,S)$ is the dimensionless function.

Using eq. (4), the mass resolution was determined versus cluster size n for the 1.5 m and 2 m lengths. Potassium (K) clusters were considered throughout the calculations since we know the velocity of the clusters [5]. For the selected parameters, the mass resolution plots are given in figure 2 for the beam source along with and perpendicular to the spectrometer axis. The parameters are taken as $V_a = 2.680$ kV, $V = 5$ kV, $v = 1000$ m/s for K clusters and $A = 11$ cm and $B = 3$ cm. $f(X,S)$ function with these parameters has a value of 1.037 and the value for $f(X,S=0)$ is 1.042 where the length L is 1.5 m. Note that practicable values from experiment are taken for the length L.

From figure 2, one can see that the resolution is much better for the perpendicular position compared with position along the beam source. With increasing n, the $m/\delta m$ values become smaller than 1000 with $n \geq 1250$. Chandezon *et al* reported similar resolution for sodium (Na) clusters having the beam source perpendicular to the axis [7]. For beam source along the axis, the resolution is relatively poor and this limits mass range to the smaller clusters. The poor resolution is due to the initial velocity. The plots also indicate that the increase of the free drift region length (L) improves the resolution, but not considerably.

In order to improve the poor resolution, the voltages V_a and V are varied, and the rest of the parameters were kept the same as in figure 2. The obtained resolution with respect to the voltage variations for $L = 1.5$ m and K_n ($n = 1$) is shown in figure 3. The resolution is better around two orders of magnitude for voltage $V_a = 8$ kV and voltage $V = 1$ kV. But, one has to notice that $f(X,S)$ function had the value of 1.037 for the results presented in figure 2.

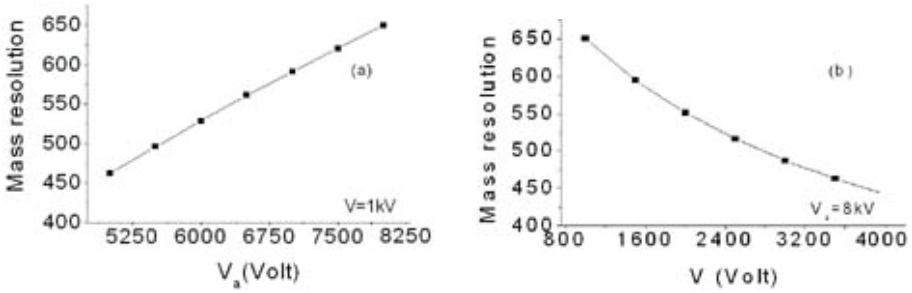

Figure 3. Mass resolution vs. voltage variation. (**a**) V_a is varied and V kept constant, (**b**) V is varied and V_a kept constant.

Table 1. $f(X, S)$ value with respect to V and V_a variation.

V_a variation			V variation		
V_a (kV)	V (kV)	$f(X, S)$ (no dim.)	V (kV)	V_a (kV)	$f(X, S)$ (no dim.)
5.0	1.0	0.772	1.0	8.0	0.679
5.5	1.0	0.754	1.5	8.0	0.760
6.0	1.0	0.737	2.0	8.0	0.814
6.5	1.0	0.721	2.5	8.0	0.852
7.0	1.0	0.706	3.0	8.0	0.882
7.5	1.0	0.692	3.5	8.0	0.905
8.0	1.0	0.679	4.0	8.0	0.925

For the results given in figure 3, we calculated the value of the function $f(X, S)$. The obtained values for the function are less than 1 (table 1). The decrease of $f(X, S)$ results in loss in spatial resolution resulting from the enlargement of the ionization region (Δx) [4,7]. The table implies that improvement of the energy resolution results in decreasing the spatial resolution.

$f(X, S)$ was scanned over the reduced parameter $X(X = x/L)$ for finding out if the value of the function can be obtained around 1 in which x is the distance measured from the last grid of the ionization position to the ionization volume. In this case, the spatial resolution can be recovered. The results presented in figure 4 illustrate that the values of the function decreases further as one shifts the ionization region to the last grid of the ionization region. This manifests that the spatial resolution cannot be recovered. Hence, the perpendicular position along with the turnaround time method provides the spectrometer with the high spatial and energy resolution.

3.2 *Time-lag energy focusing*

Time-lag focusing method is based on the idea that ions are created and then the formed ions are accelerated, hence producing time-lag τ between the formation of the ions and acceleration of the ions [1]. To describe the method in detail, we may

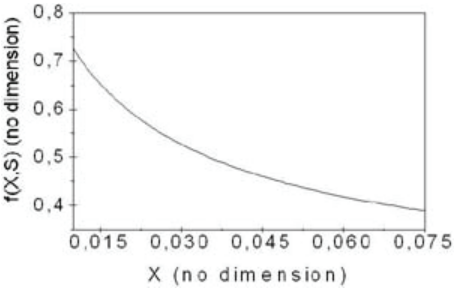

Figure 4. The $f(X, S)$ function values with the X reduced parameter.

consider three identical ions, but with initial velocities $\pm v_0$ and 0 at the position x_0, respectively. The ions will have the new positions $v_0\tau$ due to the initial velocities that produce flight time difference with respect to x_0. Without time-lag the time difference is nearly half the turnaround time ∂T_v and then using eq. (1) we get

$$T(x_0, -v) - T(x_0, 0) = T(x_0, v) - T(x_0, 0) = 2mv/qE_1. \tag{5}$$

During the time-lag, the time difference for each ion is

$$T(x_0 + v\tau, -v) - T(x_0 - 0) \approx v\tau \frac{\partial T}{\partial x}. \tag{6}$$

In order to eliminate the time difference defined by eq. (5), the change in the flight time given by eq. (6) should compensate the flight time obtained without time-lag. The requirement is as follows:

$$v\tau \frac{\partial T}{\partial x} + \frac{mv}{qE_1} = 0. \tag{7}$$

From this equation,

$$\tau = -\frac{m}{qE_1\,(\partial T/\partial x)}. \tag{8}$$

From eq. (8), the method is mass-dependent, but it is independent of velocity. Also the ion-lag focusing is possible when $\partial T/\partial x$ is negative. The positive value can result in defocusing since $\partial T/\partial x = 0$ is required for the spatial resolution [1,7].

Using eq. (8), we plotted τ as a function of cluster sizes for both perpendicular and parallel positions of the beam sources (figure 5) considering $L = 1.5$ m and $L = 2$ m. The parameters used for the plot are the same as in figure 2 to have the same spatial resolution. For the perpendicular position, the mass range up to K_{170} is within the experimental value for $L = 2$ m while the range is $1 \leq K_n \leq 85$ for $L = 1.5$ m. The mass limitation for parallel position takes place at K_{168} for $L = 2$ m and it is at K_{85} for $L = 1.5$ m. The reported experimental τ values are in the range of 0–3 μs [1]. On the one hand, this points out that the time-lag approach is a more convenient method for the parallel position of the beam source when the mass range obtained via turnaround time is taken into account (see figure 3 for the

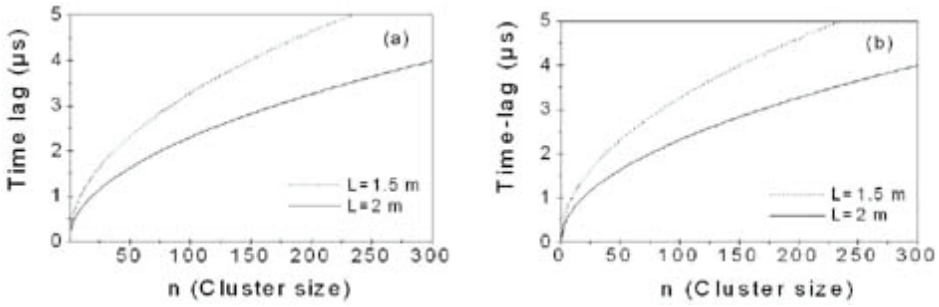

Figure 5. Time-lag changes with the cluster sizes n. (**a**) Beam source parallel to the spectrometer axis and (**b**) beam source perpendicular to the axis.

results of turnaround time). On the other hand, the method providing resolution for the perpendicular position is relatively poor compared to the turnaround time method. The mass limitation arises from the time-lag energy focusing method.

As seen from figure 5, the time-lag exceeds 3 μs beyond the cluster sizes and becomes large with increasing n. The large τ means that $\partial T/\partial x$ is very small; hence elimination of the velocity effect gets difficult [7]. The mass range can be improved via active parameter of the spectrometer, namely, V_a and V. However, this can cause decreasing spatial resolution.

4. Conclusion

From the results presented here we can conclude that within the methods used for the the energy resolution, turnaround time approach provides high resolution when the beam source is perpendicular to the spectrometer axis, but the resolution is relatively poor for the parallel position of the beam source. On the other hand, the mass range obtained via the time-lag energy focusing method shows that the approach is more appropriate for the parallel position. Hence using the methods for the energy resolution in an effective way depends on the beam source position that is the merit of this study compared to other studies [7]. The poor resolution arising from both methods can be improved, but one has to cope with the spatial resolution loss.

References

[1] W C Wiley and I H McLaren, *Rev. Sci. Instrum.* **26**, 1150 (1955)
[2] W A de Heer, *Rev. Mod. Phys.* **65**, 677 (1993)
[3] V Kasperovich, G Tikhonov, K Wong, P Brockhaus and V V Kresin, *Phys. Rev.* **A60**, 3071 (1999)
[4] Ş Şentürk, K Harigaya and O Özsoy, *Czech. J. Phys.* **55**, 1275 (2005)
[5] Ş Şentürk, J P Connerade, D D Burges and N J Mason, *J. Phys.* **B33**, 2763 (2000)
[6] W A de Heer and P Milani, *Rev. Sci. Instrum.* **62**, 670 (1991)
[7] F Chandezon, B Huber and C Ristori, *Rev. Sci. Instrum.* **65**, 3344 (1994)